NRIAG JOURNAL OF ASTRONOMY AND GEOPHYSICS
2020, VOL. 9, NO. 1, 586–597
https://doi.org/10.1080/20909977.2020.1821573

Application of natural polymers enhanced with ZnO and CuO as humidity sensor

Hend A Ezzat[a], Maroof A Hegazy[a], Nadra A Nada[b], Osama Osman[c] and Medhat A Ibrahim[c]

[a]Nano Technology Unit, Solar and Space Research Department, National Research Institute of Astronomy and Geophysics (Nano NRIAG), Helwan, Egypt; [b]Physics Department, Faculty of Women for Arts, Science and Education, Ain Shams University, Cairo, Egypt; [c]Molecular Spectroscopy and Modeling Unit, Spectroscopy Department, National Research Centre, Giza, Egypt

ABSTRACT

Metal oxides enhance the electronic properties of natural polymers. Accordingly, natural polymers modified with metal oxides show potential application as cheap easily handled sensors. Model molecules, which described the interaction cellulose (Cel), chitosan (Cs) and sodium alginate (NaAlg) and ZnO and CuO are presented. Quantitative structure analysis relationship (QSAR) parameters were calculated at PM6 for all structures. Thermodynamic properties were also computed to demonstrate the effect of nanometal oxides on natural polymer behaviour. Calculated data revealed that, Cel, Cs and NaAlg interacted with ZnO and CuO with noticeable enhancement in the electronic and thermal properties. CuO interacted with Cel and Cs through oxygen atom while NaALg recorded non-significant changes. It is concluded that the enhancement of Cel or Cs with MO produced new nanocomposite with high electronic properties and thermal stability dedicated for applications as humidity sensor.

ARTICLE HISTORY
Received 25 June 2020
Revised 12 August 2020
Accepted 6 September 2020

KEYWORDS
QSAR; natural polymer; nanometal oxides and thermodynamic properties

1. Introduction

Polymers that are the product of living organisms' metabolic reactions classified as natural polymers (NP). That kind of substance has been used for numerous applications such as binders, drug delivery, coatings and corrosion inhibitors (Umorena and Eduokb 2016). NPs, which is also termed as biopolymers, show growing concern according to their chemical, physical and biological properties. Many researchers reported about NP, their reports include chemical composition, macromolecular weights and their basic molecular and electronic configurations, as well as properties that govern the usage strategy (Charles 2007; Lin et al. 2016; Sahariah and Másson 2017; El et al. 2018). Among the amazing properties of NPs such as easy handling, abundant and formation of unique hydrogen bondingenhanced NPs show good surface-forming interaction with other molecules (Jiang et al. 2016; Kazi and Yamamoto, 2019).

Accordingly, NPs turned out to be a promising materials to be used for new different fields (Rioux et al. 2007; Gomez et al. 2009; Wang et al. 2019). NP nanocomposite matrixes also provide desirable efficiency for integrating the advantages of both organic and inorganic materials into field of electronic devices (Arena et al. 2017; Crawford et al. 1981). Polymer nanocomposites became a promising material for various applications such as sensors, microelectronic manufacturing, coatings, optical integrated circuits and adhesives (Hashim et al. 2019; Yu et al. 2019). Furthermore, polymer nanocomposites were applied also for applications as fuel cell capacitors, self-regulating heaters and actuators (Dufresne 2008, 2013; Saboktakin et al. 2011; Ashrafi and Azadi 2015; Ibrahim et al. 2019a). Hybridisation of Cel/ZnO nanocomposite has a new property for UV sensing (Mun et al. 2017; Laffleur and Röttges, 2019). In addition, Cel-based nanocomposites provide potential exciting uses as renewable electronic products (Lefatshe et al. 2017; He et al. 2018). Moreover, BaSO4/Cel nanocomposite membrane represented a novel X-ray shielding (Jianga et al. 2019).

As well, Cs nanometallic oxide matrix is one of the least used components for electrical applications according to enhancing mechanical, the dielectric properties and thermal stability (Marroquin et al. 2013; Khalid et al. 2017; Vanitjinda et al. 2019; Ibrahim et al. 2019b). The result of Cs/ZnO nano composite film indicates that the values of conductivity and dielectric constant were improved after the introduction of ZnO. (Rahman et al. 2018; Lefebvre and Gray, 2005). Similarly, NaAlg biopolymer nanocomposite with metal oxides was utilised in various applications as corrosion inhibitor and high-capacity Li-Ion batteries (Kovalenko et al. 2011; Jmiai et al. 2018; Updegraff, 1969). NP molecular modelling offers a technique to follow up electronic properties of NP. Such techniques with different levels of theories were applied to investigate different NP (Ibrahim and Mahmoud 2009; Ibrahim et al. 2011; Omar et al. 2021). In this

CONTACT Hend A Ezzat hend_ahmed16@yahoo.com Nano Technology Unit, Solar and Space Research Department, National Research Institute of Astronomy and Geophysics (Nano NRIAG), Helwan, Egypt

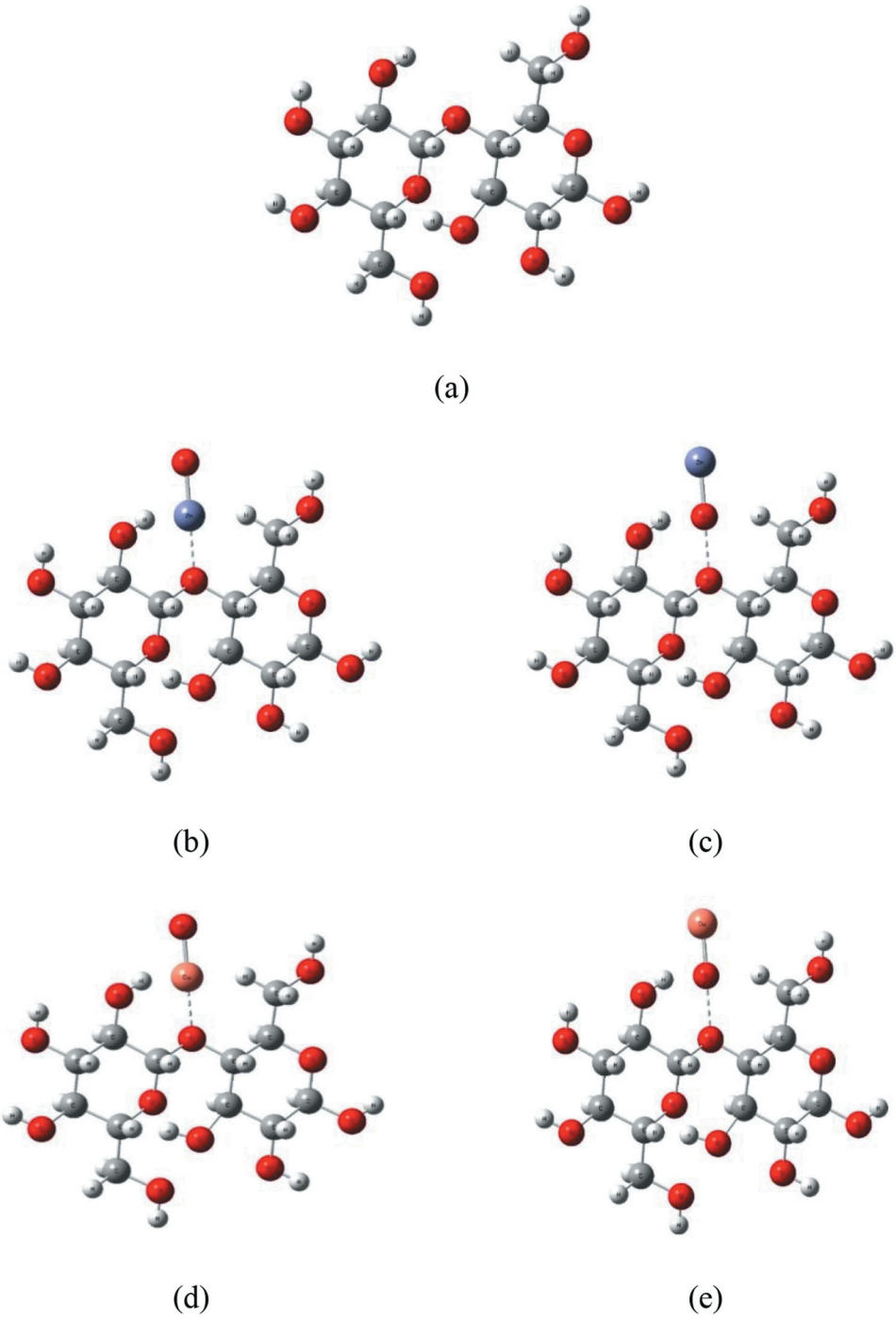

Figure 1. Caculated PM6 semiempirical quantum mechanical models for the following structures (a) Cel, (b) Cel/ZnO, (c) Cel/OZn (d) Cel/CuO and (e) Cel/OCu.

sense, QSAR is a theoretical approach in which the active molecules are evaluated and reactivity is concerned. QSAR is a calculation that studies the relationship of the chemical structure between both physicochemical property and biological activity (Hansch and Leo 1995; Welsh et al. 2007; Ibrahim and Osman, 2009). QSAR is also a significant tool for molecules, specifically those used in the chemical and biological sciences and engineering. QSAR have many structural, physical and chemical properties utilised for calculations which so-called descriptors. Furthermore, there are several popular descriptors, such as those representing the electronic effects inside molecules, the results of lipophilicity (hydrophobicity) (Elhaes et al. 2012; El-Sayed et al., 2018; Bayoumy et al. 2020).

It could be concluded that the NP could be modified for many applications among them applications as sensors. Cellulose could be modified with CuO-forming hybrid nanocomposites membranes then applied for H_2S gas detection at low temperatures (Hittini et al. 2020).

Based on the above considerations, NP such as Cel, Cs and NaAlg are modified with CuO and ZnO to

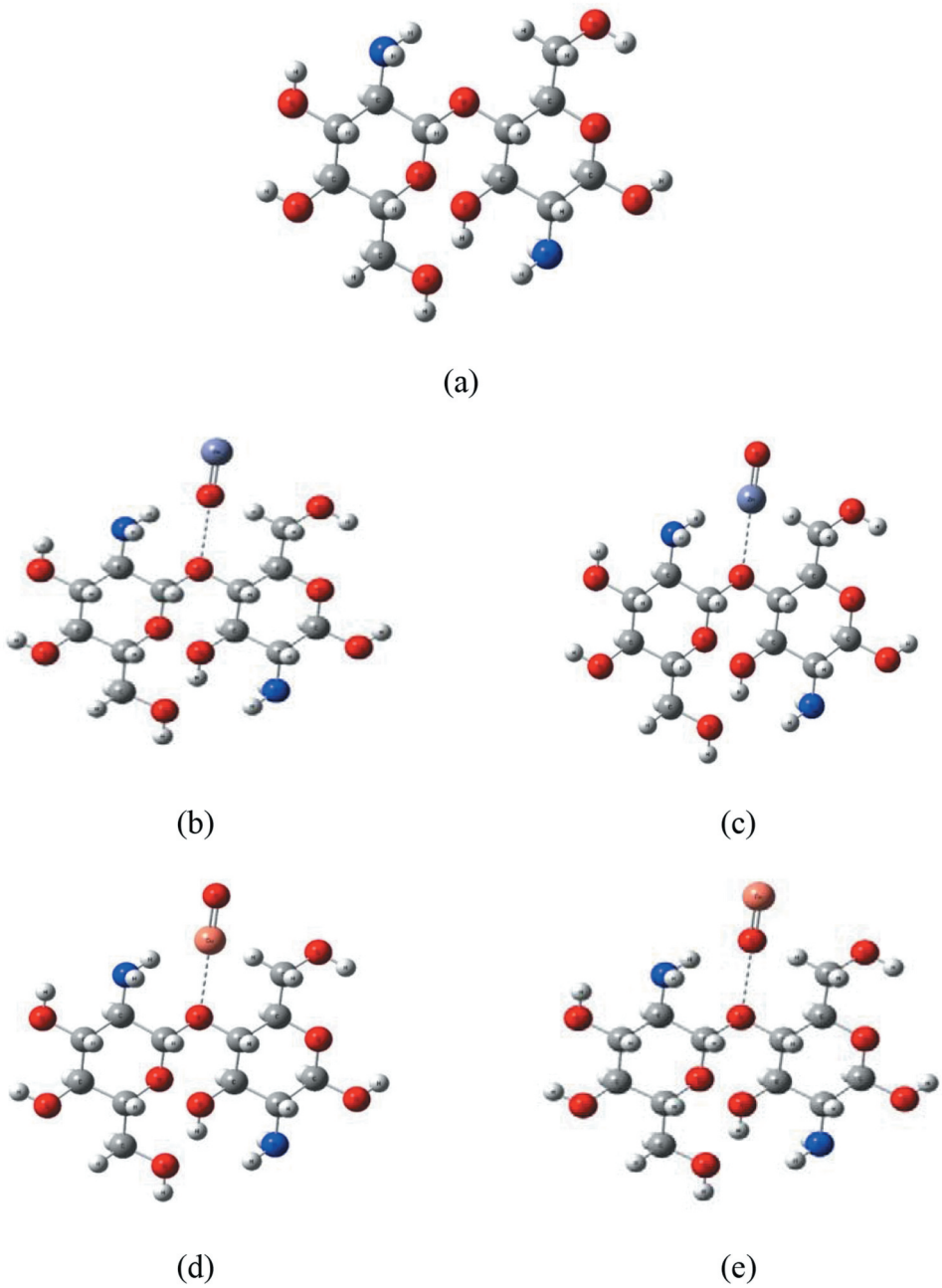

Figure 2. Caculated PM6 semiempirical quantum mechanical models for the following structures (a) Cs, (b) Cs/ZnO, (c) Cs/OZn (d) Cs/CuO and (e)Cs/OCu.

enhance their electronic properties. The scheme of interaction is indicated with molecule modelling. Then, QSAR calculations and thermodynamic properties were computed for all structures at PM6 level. Based on electronic properties, the best structure is tested as sensor for humidity.

2. Calculation details

Model structures were conducted for NP including Cel, Cs and NaAlg modified with nanometal oxides ZnO and CuO at PM6 level using SCIGRESS 3.0 soft code that it is performed at Spectroscopy Department, National Research Centre, NRC. The electronic, QSAR, and thermodynamics properties are computed for the optimised structures also at the same level. Based on the calculations, the Cs/CuO nanocomposite is chosen to interact with 3 water molecules to test it as humidity sensor.

3. Results and discussion

3.1. Building the model molecules

The first step in this study is to indicate how the model molecules are built. The choices of NP were based on their abundance, biodegradation, easy handling. While metal oxide (MO) might enhance the natural

polymers' electronic properties. Gathering both ideas the surface of the NP/MO could be acted as asensor. The mechanism of interaction between NP and MO is tried through several model structures. So that, NP interaction with nanometal oxides was considered into three groups. The three groups that represent this interaction are Cel group, Cs group and NaAlg group with nano metal oxides as ZnO and CuO. Nanometal oxides interaction with NP supposed through the oxygen atom -O- which links the units of polymer chain as adsorb state. Nanometal oxides interacted through metal atom once and through the oxygen atom once. NP groups Cel, Cs and NaAlg and its nanometal oxides adsorption represented in Figures1, 2 and 3, respectively. The electronic, QSAR, and thermodynamics properties of all simulated groups were computed at PM6 level.

3.2. QSAR calculations

The supposed three model groups were optimised to reflect physical electronic and QSAR properties. The outcome properties are listed in Table 1. These properties were functionalised as charge, total energy (TE), molecular orbital energy gap (ΔE), total dipole moment (TDM) and ionisation potential (IP), Log P, molar refractivity (MR), surface area and volume.

First, descriptor is charge were equal to zero for all model molecules that all structures were in ground

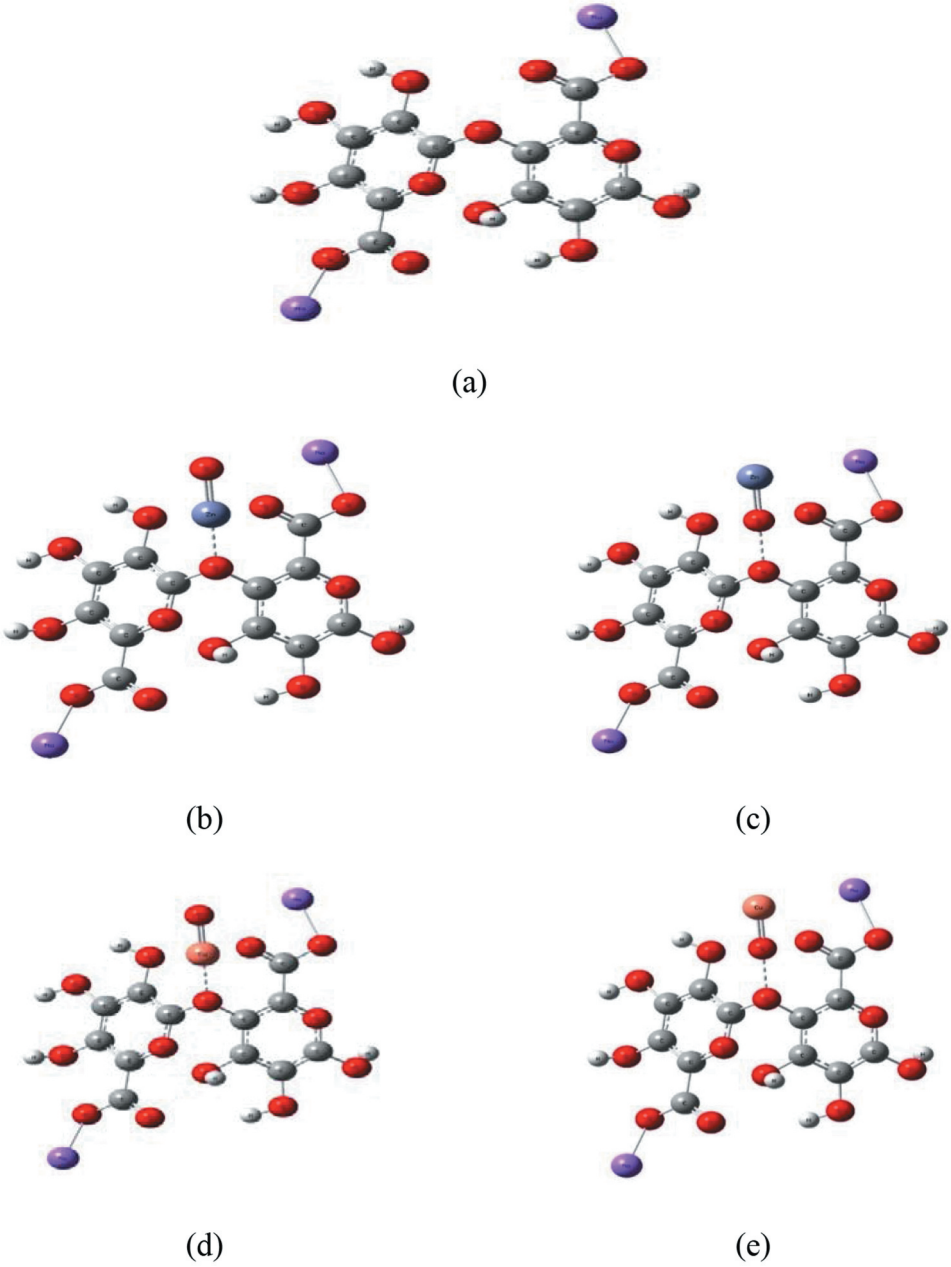

Figure 3. Caculated PM6 semiempirical quantum mechanical models for the following structures (a) NaAlg, (b) NaAlg/ZnO, (c) NaAlg/OZn (d) NaAlg/CuO and (e) NaAlg/OCu.

Table 1. Calculated properties using semiempirical theory at PM6 level as Charge, Total Energy(ev), Dipole moment (Debye), Ionisation potential (eV) and Log P for the three groups of natural polymer with metal oxides:Cel, Cel/ZnO,Cel/OZn, Cel/CuO, Cel/OCu, Cs, Cs/ZnO, Cs/OZn, Cs/CuO, Cs/OCu, NaAlg, NaAlg/ZnO, NaAlg/OZn, NaAlg/CuO and NaAlg/OCu.

Structure	Charge	T E (ev)	ΔE	TDM (Debye)	IP(eV)	Log P	MR	MW	Surface Area	Volume
Cel	0	−5927.075	10.723	2.175	−10.524	−2.977	68.337	342.296	300.63	257.36
Cel/ZnO	0	−6289.463	6.338	2.793	−10.302	−3.328	69.780	423.705	349.35	297.5
Cel/OZn	0	−6281.369	6.279	1.771	−9.055	−3.328	69.780	423.705	337.42	297.53
Cel/CuO	0	−7401.521	5.399	7.784	−5.866	−3.328	69.780	421.842	316.25	282.13
Cel/OCu	0	−7239.899	7.389	11.767	−3.918	−3.328	69.780	421.842	335.17	282.33
Cs	0	−5776.180	10.218	3.877	−9.806	−3.672	71.652	340.327	312.2	268.56
Cs/ZnO	0	−6140.246	6.583	2.998	−9.920	−4.023	73.095	421.735	349.49	302.87
Cs/OZn	0	−6131.391	6.287	4.968	−8.614	−4.023	73.095	421.735	350.89	308.61
Cs/CuO	0	−7274.730	4.712	5.911	−6.729	−4.023	73.095	419.872	351.48	296.08
Cs/OCu	0	−7083.695	7.271	6.500	−6.779	−4.023	73.095	419.872	352.34	296.46
NaAlg	0	−6332.076	8.916	9.202	−9.260	−2.536	66.216	414.227	284.76	251.56
NaAlg/ZnO	0	−6844.882	6.709	16.929	−9.636	−2.887	67.659	495.636	332.42	286.52
NaAlg/OZn	0	−6859.850	7.725	6.863	−8.848	−2.887	67.659	495.636	340.52	294.91
NaAlg/CuO	0	−7936.236	5.623	8.592	−6.308	−2.887	67.659	493.773	320.56	280.08
NaAlg/OCu	0	−7727.784	6.521	7.294	−6.062	−2.887	67.659	493.773	328.44	281.10

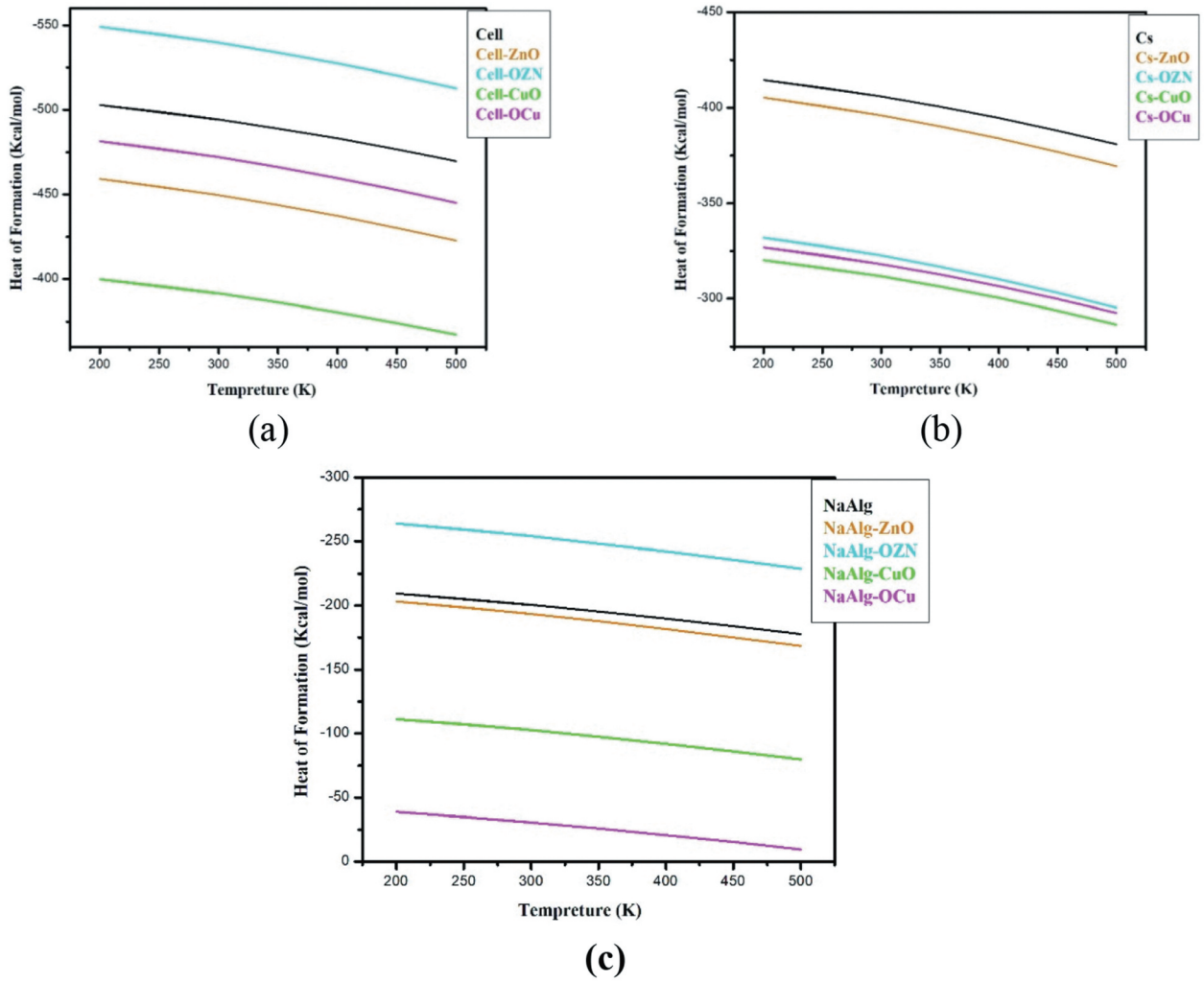

Figure 4. PM6 calculated heat of formation (kcal/mol) as a function of temperature (K) of Cel and Cel/MO (b) Cs and Cs/MO (c) NaAlg and NaAlg/MO.

state. After that, TE was computed for representing the stability of the structures. When TE decreases the structure classified as more stable compound. As mentioned in table 1 TE for Cel group, TE for Cel was equal −5927.075 eV. Furthermore, TE changed with nanometal oxide adsorption as decreasing for Cel/ZnO, Cel/OZn, Cel/CuO and Cel/OCu to −6289.463, −6281.369, −7401.521 and −7239.899 eV, respectively, that the lowest value of TE was for Cel/CuO which is the most stable structure in this group. For Cs group

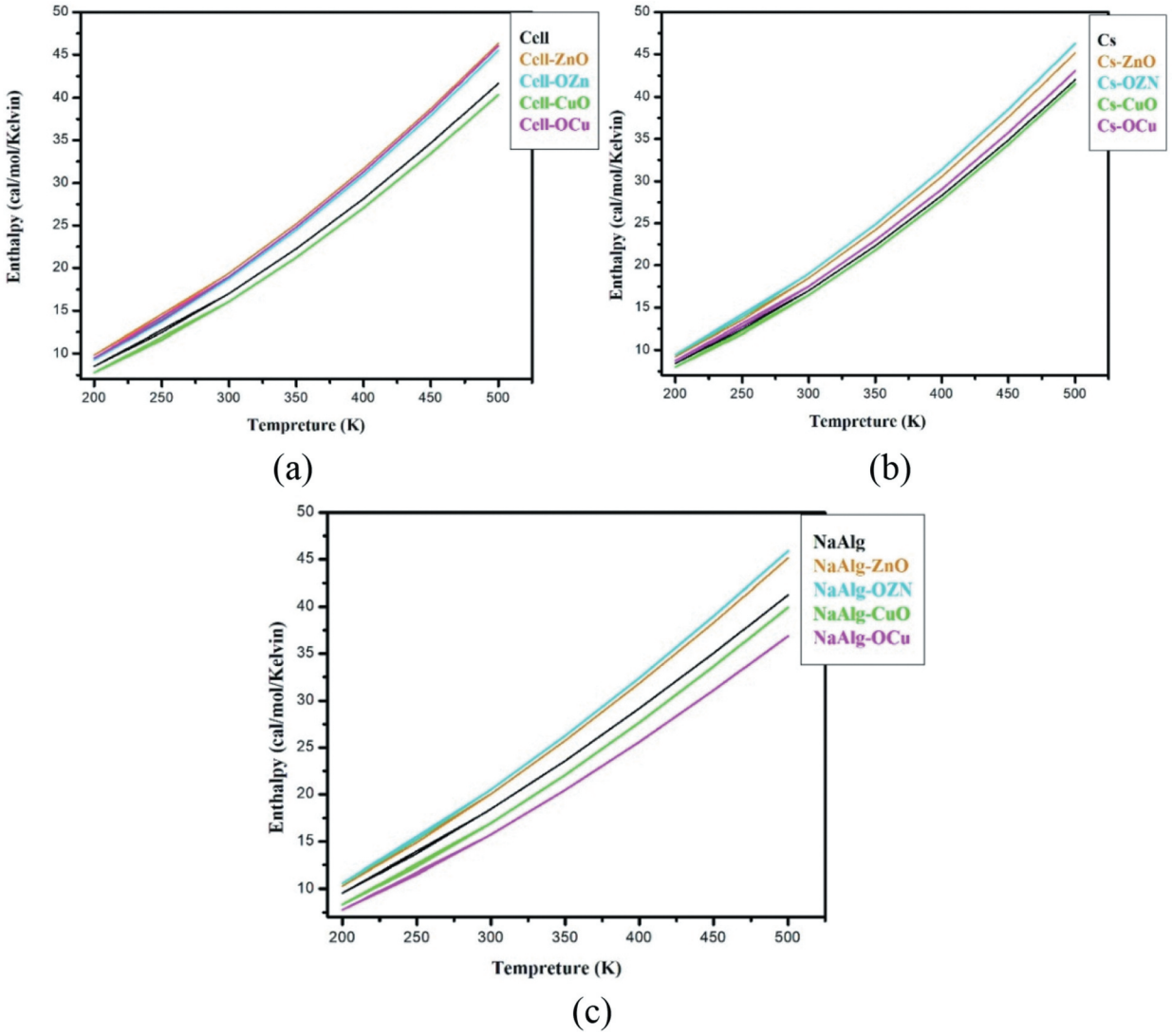

Figure 5. PM6 calculated Enthalpy (cal/mol/K) as a function of temperature (K) of (a) Cel and Cel/MO (b) Cs and Cs/MO (c) NaAlg and NaAlg/MO.

also TE changed from −5776.180 eV to −6140.246, −6131.391, −7274.730 and −7083.695 eV for Cs/ZnO, Cs/OZn, Cs/CuO and Cs/OCu, respectively, which means that Cs/CuO is the most stable structure in this group according to the lowest value of TE. Similarly, TE for NaAlg group changed that the lowest value of TE and most stable structure was for NaAlg/CuO that equal −7936.236 eV.

Second descriptor was the band gap energy ΔE that when the band gap decreases the structure became more reactive. For Cel group band gap ΔE for Cel 10.723 eV decreased when it interacted with nano metal oxides that the lowest value was for Cel/CuO 5.399 eV. Also, Cs group band gap energy ΔE affected by adding nano metal oxides that the lowest value was for Cs/CuO 4.712 eV. Equally, NaAlg group band gap energy ΔE decreased from 8.916 to 5.623 eV, respectively, that the lowest value was for NaAlg/CuO.

Moreover, TDM is a descriptor, which describes compound reactivity that the highest TDM, the more reactive compound. Nano metal oxides increase TDM for all studied natural polymer Cel, Cs and NaALg, which means that reactivity increased for NP/MO. These results indicated that MO effect on NP electronic properties positively specially NP/CuO.

Other important QSAR descriptor is IP, which characterises compound reactivity. IP defined as the needed energy for compound to be ionised. The reactivity of chemical compounds increases as IP value decreases. From data interaction of ZnO with NP, does not make a significant change in IP.

The descriptor, which describes hydrophilicity of the chemical compound, is the logarithm of the partition coefficient (log P). log P represents the proportional to the ratio of dissolving material in organic solvent to that dissolving in aqueous solvents, thus, positive Log P values apply to hydrophobic compounds, and negative values suggest hydrophilic compounds. For our group materials, all proposed structures have negative log P that the compounds

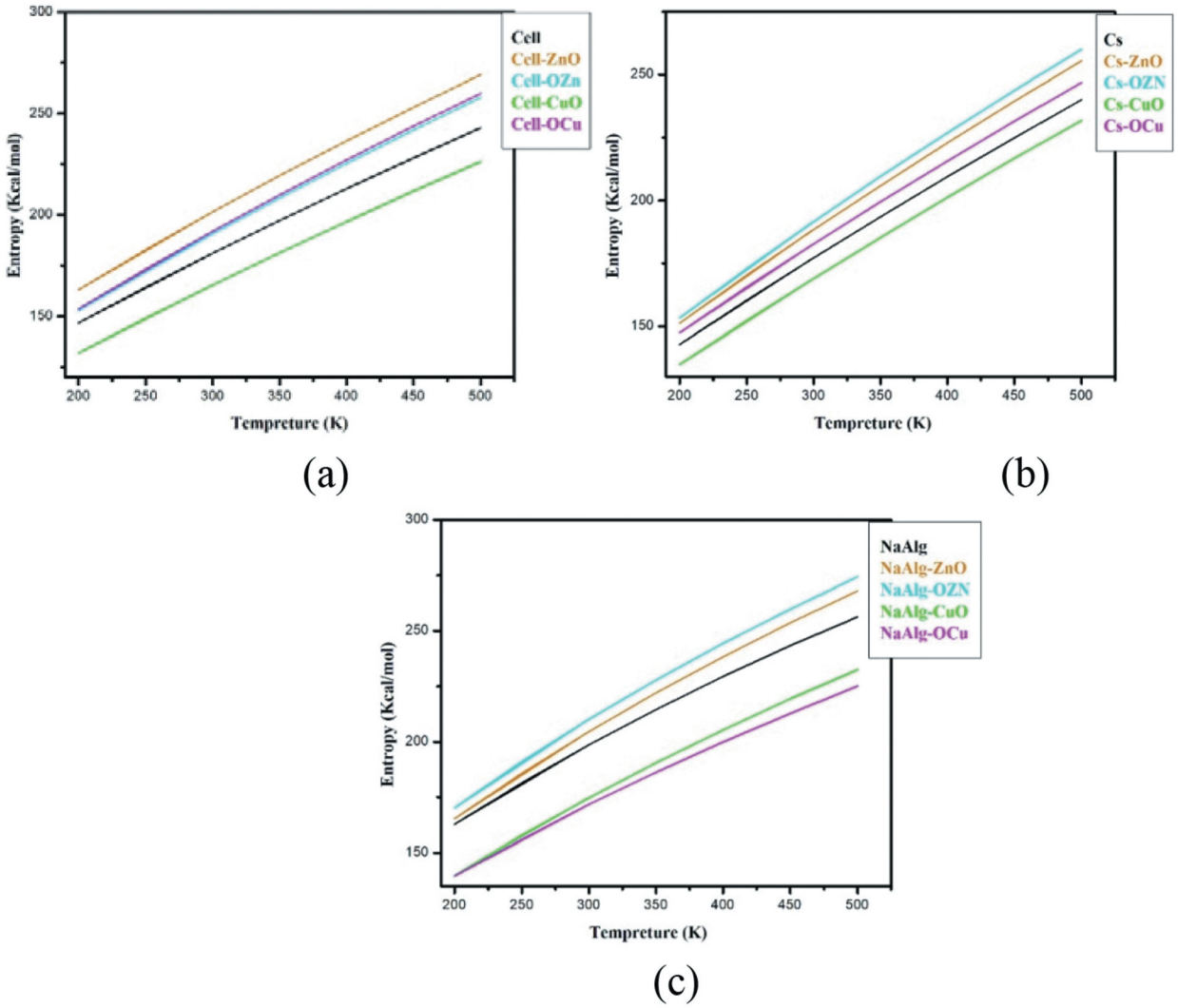

Figure 6. PM6 calculated Entropy (K cal/mol) as a function of temperature (K) of (a) Cel and Cel/MO (b) Cs and Cs/MO (c) NaAlg and NaAlg/MO.

are hydrophilic (water soluble). Subjected NPs with nano metal oxides are more hydrophilic than NP alone.

Surface area and volume are also geometrical QSAR parameters. Additionally, MR is a descriptor measure the overall polarisability of the mole of the material. The bigger the structure's molar refractivity, the greater its reactivity. As mentioned in table 1 NP with ZnO in the two different positions are more reactive than CuO interaction.

3.3. Thermodynamic properties

Heat of formation, enthalpy, entropy, free energy and heat capacity as thermal parameters were calculated for all model groups using PM6 at temperature range from 200 to 500 Kelvin. The calculated parameters are important for describing the physical behaviour of a system, in terms of its possible interaction with its surrounding media in the presence of heat. They are also indicators for a given chemical structure for its ability, behaviour when it is subjected and/or exchange heat with or from its surroundings.

The heat of formation is an important thermal descriptor, which defined as the energy emitted as heat as atoms situated at potentially infinite distances, bind and create a molecule of interest. So far as the heat of formation is concerned, it can be described as the shift in the enthalpy following the production of one mole of a material from its components in their normal and stable states, under atmospheric standard conditions at a given temperature. For the heat of formulation, for a given product, it is known as the volume of heat formed or absorbed into a single mole. Figure 4 characterises the heat of formation as a function of temperature for the three groups of NP/MO. For Cel group, heat of formation for Cel/OZn is the lowest value that it needs small amount of energy to be formed. On other hand, Cs group the lowest heat of formation was for Cs and Cs/ZnO. Similarly, NaAlg group has lowest heat of formation for NaAlg/OZn.

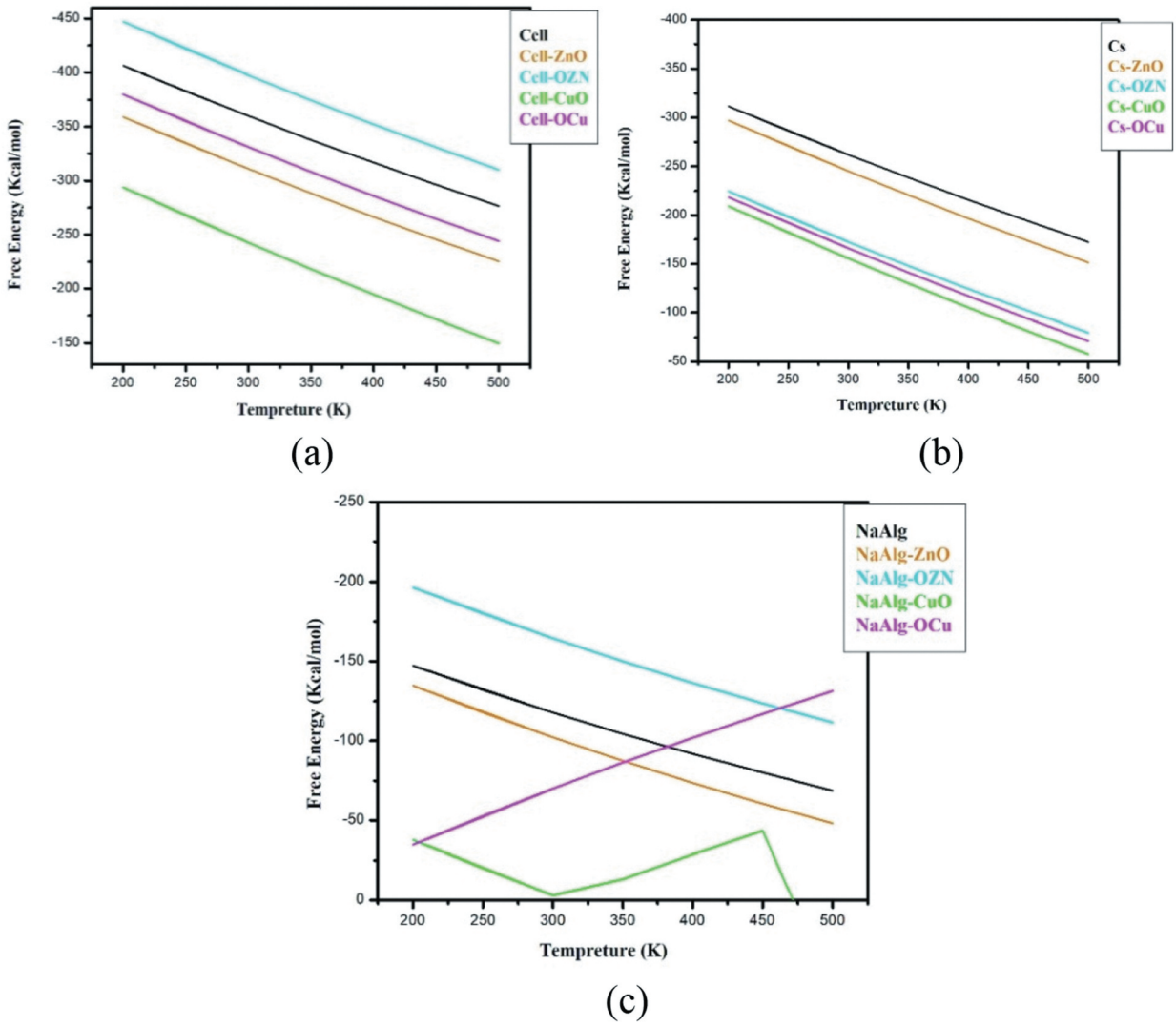

Figure 7. PM6 calculated Free energy (K cal/mol) as a function of temperature (K) of (a) Cel and Cel/MO (b) Cs and Cs/MO (c) NaAlg and NaAlg/MO.

Enthalpy is another thermal parameter that is a measurement of system's total energy. Figure 5 represents the relation of enthalpy with temperature for the studied models. For Cel group enthalpy of Cel/ZnO, Cel/OZn and Cel/OCu increased and equalled to each other. Also, Cs/OZn, Cs/ZnO and Cs/OCu enthalpy increased rather than others. Then NaAlg/OZn and NaAlg/ZnO are the highest values of group enthalpy. Beside enthalpy of all structures, structures increase with increasing temperature.

The entropy is then a function of the amount of different forms in which the structure may be organised. Figure 6 shows the entropy calculations for all model structures that the entropy for all structures increases with increase in temperature . Cel/ZnO, Cel/OZn and Cel/OCu are higher in entropy than the others. Also, Cs/OZn, Cs/ZnO and Cs/OCu are higher than Cs and Cs/CuO, respectively. In case of NaAlg group, entropy of NaAlg/OZn and NaAlg/ZnO are the highest.

The energy required in system to be effort to do work defined as free energy. The structures free energy calculations are shown in Figure 7. As shown, Cel group free energy behaviour as free energy decreased as temperature increased while Cel/OZn was the highest values. Then, Cs group recorded thesame behaviour of Cel group generally. But NaAlg group behaved differently, that free energy of NaAlg/OZn, NaAlg and NaAlg/ZnO were decreased with temperature increase while NaAlg/OCu free energy increase with temperature and NaAlg/CuO has unstable behaviour.

Other important thermal parameter is heat capacity, which is proportional to the amount of energy needed to raise its temperature by one degree. The heat capacity of subjected model structures was introduced in Figure 8. The lowest heat capacity for Cel group is Cel/CuO while the lowest heat capacity for Cs group is Cs/CuO. NaAlg group lowest value of heat capacity was for NaAlg/OCu.

4. NP/MO as humidity sensor

Correlating the studied physical as well as chemical parameters, it is clear that the great change in the

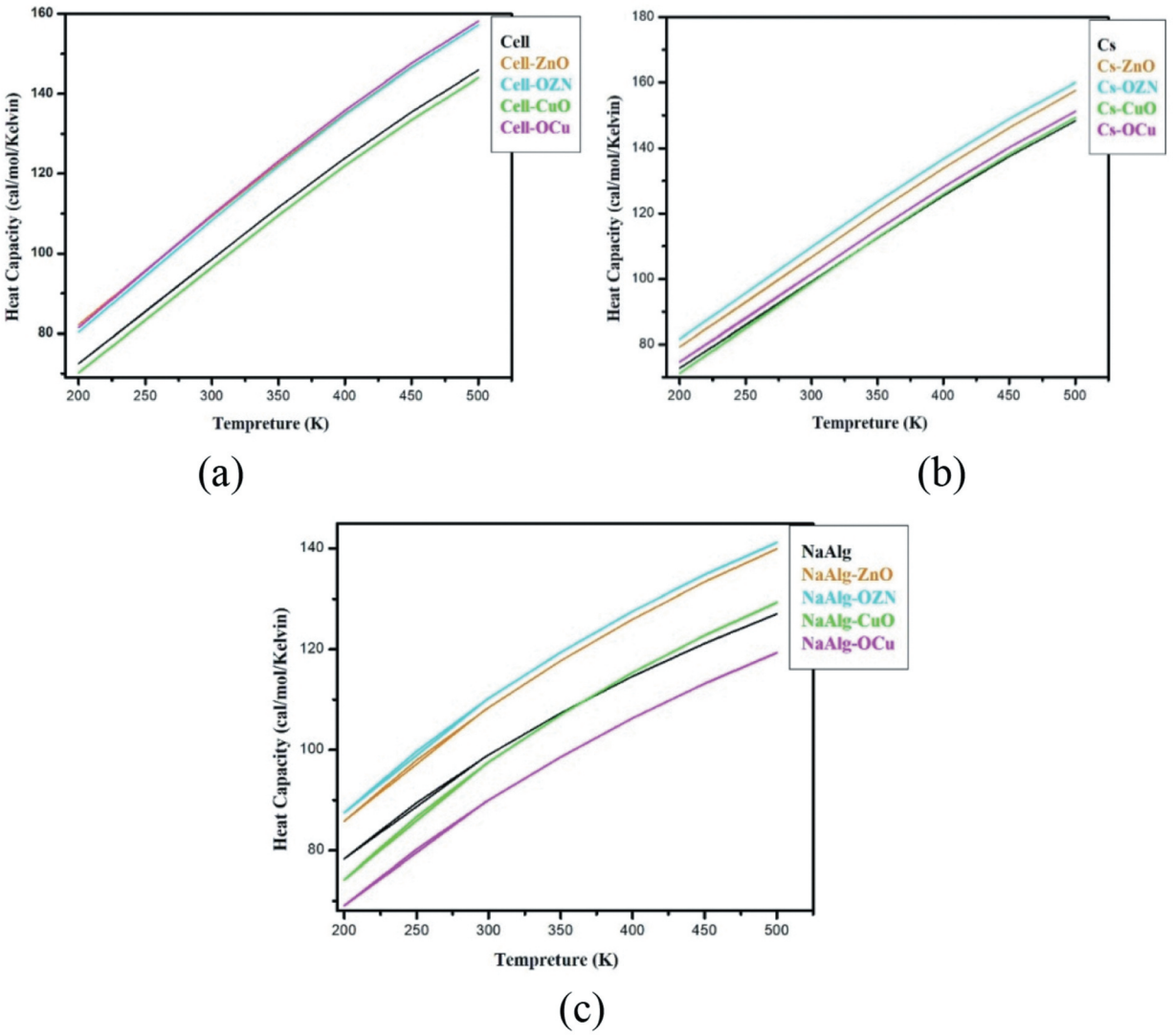

Figure 8. PM6 calculated heat capacity (cal/mol/K) as a function of temperature (K) of (a) Cel and Cel/MO (b) Cs and Cs/MO (c) NaAlg and NaAlg/MO.

electronic properties was corresponding to Cs/CuO composite. So that, the Cs/CuO composite was chosen as sensing material based on their unique electronic properties. In order to test it as sensor for humidity 3 water molecules are supposed to interact with Cs/CuO surface as indicated in Figure 9. It is worth to mention that, the processes of measuring and controlling humidity are essential issue for numerous applications (Manikandan et al. 2019). In the present work, the sensing mechanism to detect humidity with Cs/CuO depends on the change in the studied physical properties. It is stated earlier that the change in the total dipole moment as well as HOMO/LUMO band gap energy are good descriptors for reactivity of the studied surface (Ibrahim and El-Haes 2005; Ibrahim and Mahmoud 2009). So that, physical properties for example total dipole moment will be calculated for Cs/CuO before and after interaction with water molecules. The change in the calculated physical properties will be a measure for the ability of such surface to detect humidity.

The interactions reveal that the total dipole moment is increased from 5.911 to 6.959 Debye. This is an indication that the studied polymer modified with MO could act as sensor for humidity. The thermal stability ensures that the existence of the MO in the composite enhanced the stability of the structure.

5. Conclusion

The conducted structure of natural polymer (Cel, Cs and NaAlg) interaction with some nanometal oxides ZnO and CuO through the oxygen atom, which linked the two unit with nanometal oxides once from oxygen atom and other from metal atom (Zn,Cu) were studied to find out the effect of nano MO on NP in enhancing electronic and thermal properties. QSAR calculations and thermodynamic property calculations indicated that PM6 could describe the interaction stability of NP with MO accurately. All result specified that NP (Cel, Cs and NaAlg) interaction with MO (ZnO and CuO) could be occurred and enhanced NP electronic properties and thermal

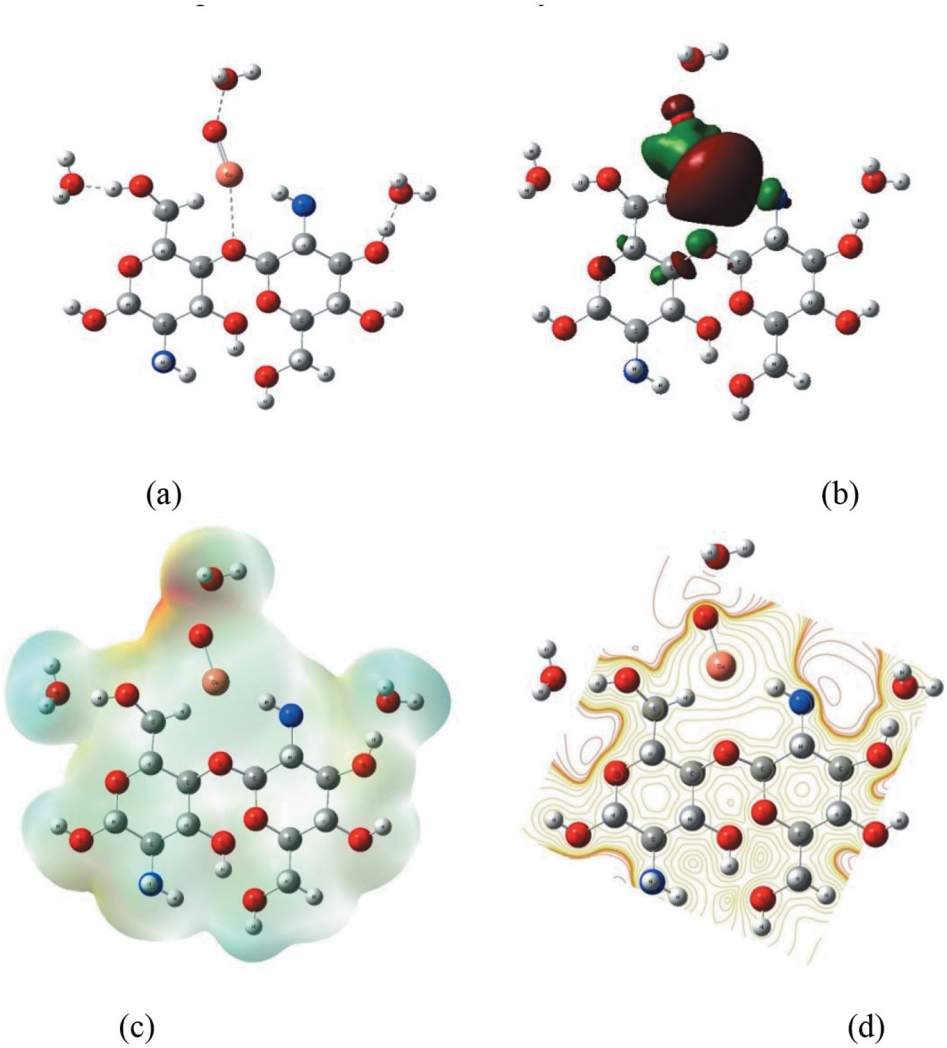

Figure 9. PM6 calculated model structures for (a) Cs/CuO.3H_2O, (b) HOMO/LUMO orbital's for Cs/CuO.3H_2O, (c,d) Mapping MESP Cs/CuO.3H_2O.

properties. The most effective MO was CuO interacted with Cel and Cs through oxygen atom while NaAlg recorded non-significant changes. Accordingly, enhancing Cel or Cs with MO produced new nanocomposite with high electronic properties and thermal stability to be used in various electronic and sensing applications.

Possible interaction between Cs/CuO and water molecules as an application example indicated the ability of Cs/CuO to act as humidity sensor. Furthermore, it is indicated that the introduction of MO to the NP is enhancing its ability to act as cheap easily handled sensor for humidity. The presented sensor is cheap, easily handled humidity sensor for assessment for increasing the level of humidity. It is worth to mention that humidity assessment is important in space application also in cultural heritage museums whereas increasing the level of humidity is affecting the process and contents there.

Disclosure statement

No potential conflict of interest was reported by the authors.

ORCID

Hend A Ezzat http://orcid.org/0000-0002-2370-3038
Osama Osman http://orcid.org/0000-0002-9977-3964
Medhat A Ibrahim http://orcid.org/0000-0002-9698-0837

References

Arena A, Scandurra G, Ciofi C. 2017. Copper oxide chitosan nanocomposite: characterization and application in non-enzymatic hydrogen peroxide sensing. Sensors-Basel. 17(10):2198.

Ashrafi H, Azadi A. 2015. Chitosan-based hydrogel nanoparticle amazing behaviors during transmission electron microscopy. Int J Biol Macromol. 84:31–34.

Bayoumy AM, Refaat A, Yahia IS, Zahran HY, Elhaes H, Ibrahim MA, Mohd S. 2020. Functionalization of graphene quantum dots (GQDs) with chitosan biopolymer for biophysical applications. Opt Quant Electron. 52 (1):52–68.

Charles AB. 2007. Vacuum deposition onto webs, films, and foils. William Andrew, Elsevier; p. 8155.

Crawford RL. 1981. Lignin biodegradation and transformation. New York: John Wiley and Sons; p. 154.

Dufresne A. 2008. Polysaccharide nano crystal reinforced nanocomposites. Can J Chem. 86(6):484–494.
Dufresne A. 2013. Nanocellulose: a new ageless bionanomaterial. Mater Today. 16(6):220–227.
El Knidri H, Belaabed R, Addaou A, Laajeb A, Lahsini A. 2018. Extraction chemical modification and characterization of chitin and chitosan. Int J Biol Macromol. 120:1181–1189.
Elhaes H, Osman O, Ibrahim M. 2012. Interaction of nano structure material with heme molecule: modelling approach. J Comput Theor Nanosci. 9(7):901–905.
El-Sayed M, Omar A, Bayoumy AM, Ibrahim M. 2018. Chitosan ibuprofen interaction: modeling approach. Sens Lett. 16(5):1–9.
Gomez CG, Pérez Lambrecht MV, Lozano JE, Rinaudo M, Villar MA. 2009. Influence of the extraction–purification conditions on final properties of alginates obtained from brown algae (Macrocystis pyrifera). Int J Biol Macromol. 44(4):365–371.
Hansch C, Leo L. 1995. Exploring QSAR: fundamentals and applications in chemistry and biology. Washington: American Chemical Society.
Hashim A, Al-Attiyah KHH, Obaid H. 2019. Modern developments of polymer blend/oxide nanocomposites for biomedical applications as antibacterial and radiation shielding materials: a review. Res J Agric & Biol Sci. 14 (1):8–18.
He Ch, Huang J, Li S, Meng K, Zhang L, Chen Z, Lai Y. 2018. Mechanically resistant and sustainable cellulose-based composite aerogels with excellent flame retardant, sound-absorption, and superantiwetting ability for advanced engineering materials. ACS Sustainable Chem Eng. 6(1):927–936.
Hittini W, Abu-Hani AF, Reddy N, Mahmoud ST. 2020. Cellulose-copper oxide hybrid nanocomposites membranes for H2S gas detection at low temperatures. Sci Rep. 10:2940.
Ibrahim ID, Jamiru T, Sadiku ER, Hamam Y, Alayli Y, Eze AA. 2019a. Application of nanoparticles and composite materials for energy generation and storage. IET Nanodielectr. 2(4):115–122.
Ibrahim ID, Jamiru T, Sadiku ER, Hamam Y, Alayli Y, Eze AA. 2019b. Application of nanoparticles and composite materials for energy generation and storage. ET Nanodielectrics. 2(4):115–122.
Ibrahim M, El-Haes H. 2005. Computational spectroscopic study of copper, cadmium, lead and zinc interactions in the environment. Int J Environ Pollut. 23:417–424.
Ibrahim M, Mahmoud -A-A. 2009. Computational notes on the reactivity of some functional groups. J Comput Theor Nanosci. 6:1523–1526.
Ibrahim M, Osman O. 2009. Spectroscopic analyses of cellulose: fourier transform infrared and molecular modelling study. J Comput Theor Nanosci. 6(5):1054–1058.
Ibrahim M, Osman O, Mahmoud -A-A. 2011. Spectroscopic analyses of cellulose and chitosan: FTIR and modeling approach. J Comput Theor Nanosci. 8(1):117–123.
Jiang Z, Zhang Z, Song J, Meng Q, Zhou H, He Z, Han B. 2016. Catalyzed efficient conversion of cellulose to oxalic acid in alkaline solution under low oxygen pressure. ACS Sustainable Chem Eng. 4(1):305–311.
Jianga X, Zhua X, Chang C, Liuc S, Luoad X. 2019. X-ray shielding structural and properties design for the porous transparent BaSO4/cellulose nanocomposite membranes. Int J Biol Macromol. 139:793–800.
Jmiai A, El Ibrahimi B, Tara A, El Issami S, Jbara O, Bazzi L. 2018. Alginate biopolymer as green corrosion inhibitor for copper in 1 M hydrochloric acid: experimental and theoretical approaches. J Mol Struct. 1157:408–417.
Kazi GAS, Yamamoto O. 2019. Effectiveness of the sodium alginate as surgical sealant materials. Wound Med. 24 (1):18–23.
Khalid A, Khan R, Ul-Islam M, Khn T, Wahid F. 2017. Bacterial cellulose-zinc oxide nanocomposites as a novel dressing system for burn wounds. Carbohydr Polym. 164:214–221.
Kovalenko I, Zdyrko B, Magasinski A, Hertzberg B, Milicev Z. 2011. A major constituent of brown algae for use in high-capacity Li-Ion batteries. Sci. 334 (6052):75–79.
Laffleur F, Röttges S. 2019. Mucoadhesive approach for buccal application: preactivated chitosan. Eur Polym J. 113:60–66.
Lefatshe K, Muiva CM, Kebaabetswe LP. 2017. Extraction of nanocellulose and in-situ casting of ZnO/cellulose nanocomposite with enhanced photocatalytic and antibacterial activity. Carbohydr Polym. 164:301–308.
Lefebvre J, Gray DG. 2005. AFM of adsorbed polyelectrolytes on cellulose I surfaces spin-coated on silicon wafers. Cellulose. 12:127–134.
Lin T, Liu E, He H, Shin MC, Moon C, Yang VC, Huang Y. 2016. Nose-to-brain delivery of macromolecules mediated by cell-penetrating peptides. Acta Pharm Sin B. 6(4):352–358.
Manikandan V, Tudorache F, Petrila I, Mane RS, Kuncser V, Vasile B, Morgan D, Vigneselvan S, Mirzaei A. 2019. Fabrication and characterization of Ru-doped Li Cu Fe_2O_4 nanoparticles and their capacitive and resistive humidity sensor applications. J Magn Magn Mater. 474:563.
Marroquin JB, Rhee KY, Park SJ. 2013. Chitosan nanocomposite films: enhanced electrical conductivity, thermal stability, and mechanical properties. Carbohydr Polym. 92(2):1783–1791.
Mun S, Ch. KH, Ko H-U, Zhai L, Kim JW, Kim J. 2017. Flexible cellulose and ZnO hybrid nanocomposite and its UV sensing characteristics. Sci Technol Adv Mater. 18 (1):437–446.
Omar A, Ezzat H, Elhaes H, Ibrahim MA. 2021. Molecular modeling analyses for modified biopolymers. Biointerface Res Appl Chem. 11(1):7847–7859.
Rahman PM, Mujeeb VA, Muraleedharan K, Thomas SK. 2018. Chitosan/nano ZnO composite films: enhanced mechanical, antimicrobial and dielectric properties. Arabian J Chem. 11(1):120–127.
Rioux LE, Turgeon SL, Beaulieu M. 2007. Characterization of polysaccharides extracted from brown seaweeds. Carbohydr Polym. 69(3):530–537.
Saboktakin MR, Tabatabaie RM, Maharramov A, Ramazanov MA. 2011. Synthesis and characterization of pH-dependent glycol chitosan and dextran sulfate nanoparticles for effective brain cancer treatment. Int J Biol Macromol. 49(4):747–751.
Sahariah P, Másson M. 2017. Antimicrobial chitosan and chitosan derivatives: a review of the structure-activity relationship. Biomacromolecules. 18(11):3846–3868.
Umorena SA, Eduokb UM. 2016. Application of carbohydrate polymers as corrosion inhibitors for metal substrates in different media: A review. Carbohydr Polym. 140:314–341.

Updegraff DM. 1969. Semimicro determination of cellulose in biological materials. Anal Biochem. 32 (3):420–424.

Vanitjinda G, Nimchua T, Sukyai P. 2019. Effect of xylanase-assisted pretreatment on the properties of cellulose and regenerated cellulose films from sugarcane bagasse. Int J Biol Macromol. 122:503–516.

Wang X, Zhang Y, Liang H, Zhou X, Luo Y. 2019. Synthesis and properties of castor oil-based waterborne polyurethane/sodium alginate composites with tunable properties. Carbohydr Polym. 208:391–397.

Welsh WJ, Tong W, Georgopoulos PG. 2007. Toxic informatics: an introduction in: computational toxicology: risk assessment for pharmaceutical and environmental chemicals. In:: Ekins S, editor. New Jersey: John Wiley & Sons, Inc; p. 151–181.

Yu S, Xu X, Feng J, Liu M, Hu K. 2019. Chitosan and chitosan coating nanoparticles for the treatment of brain disease. Int J Pharm. 560:282–293.